



Volume: 2, Issue: 10, 549-555
Oct 2015
www.allsubjectjournal.com
e-ISSN: 2349-4182
p-ISSN: 2349-5979
Impact Factor: 5.742

Arash Tahmasebifar

a) Department of Molecular
Medicine & Nanomedicine,
Faculty of Advanced Medical
Technologies, Golestan
University of Medical
Sciences (GOUMS), Iran.
b) Kimia Medical Center,
Golestan University of
Medical Sciences (GOUMS),
Iran.

Kimia Tahani

Student Research
Committee, Golestan
University of Medical
Sciences (GOUMS), Iran.

Reza Ghanbari

Department of Molecular
Medicine & Nanomedicine,
Faculty of Advanced Medical
Technologies, Golestan
University of Medical
Sciences (GOUMS), Iran.

Leila Haghshenas

Department of cellular and
Molecular Biology,
International University of
Spain, Madrid, Spain &
Department of Clinical
Research Apheta Institute of
India, New Delhi, India.

Majid Shahbazi

Department of Molecular
Medicine & Nanomedicine,
Faculty of Advanced Medical
Technologies, Golestan
University of Medical
Sciences (GOUMS), Iran.

Correspondence

Arash Tahmasebifar

Department of Molecular
Medicine & Nanomedicine,
Faculty of Advanced Medical
Technologies, Golestan
University of Medical
Sciences (GOUMS), Iran.

Cancer biomarkers detection using tracer nanoparticles and advanced nanoscopic scanning

Arash Tahmasebifar, Kimia Tahani, Reza Ghanbari, Leila Haghshenas, Majid Shahbazi

Abstract

Background: New advances in the field of molecular medicine and the discovery of novel diagnostic and therapeutic approaches to cancer diseases will depend on identifying biomolecular structures and behaviors. Using advanced nano-detection devices, nanomedicine can provide a new insight into obtaining single-molecule analysis of functionalized biomolecules or biomarkers in human malignant disorders. Because of the critical biological functions of small non-coding RNA oligonucleotides, accurate nanoscopic identification of miRNA-21 molecule was supposed to be performed.

Methods: To this end, gold nanorods (GNRs) as tracer particles with cationic surfaces were employed to label anionic miRNA-21 after normalization. Their successful interaction was approved by an average hydrodynamic diameter and surface zeta-potential test using dynamic light scattering (DLS). Then, the structural changes of the samples were investigated through scanning tunneling microscopy (STM) with a single atomic resolution.

Results: The DLS results to investigate whether GNRs could efficiently label miRNA indicated affinity of CTAB-coated GNRs to miRNA-phosphate groups in the complexes. The high qualities of STM 2-D and 3-D nanographs of GNRs and GNRs-miRNA complexes demonstrated significant differences in morphologies, placing arrangements, surfaces, sizes, and aspect ratios.

Conclusion: Following the observed direct effects of the targeted biomarkers on the tracer gold nanoparticles, we introduced a new insight into biomedical agent nanocharacterization of molecular confrontation using a newer nanoscopic application. These findings can develop nanodiagnostic and prognostic techniques such as miRNAs detection in cancer diseases via advanced scanning nanotechnology and nanocolorimetric assay.

Keywords: Gold nanorods, Cancer biomarkers, microRNA-21, Scanning tunneling microscopy.

1. Introduction

Nano-molecular medicine aims at using biological components via advanced nano-technique to identify nano-biomolecular characteristics and structure for which an innovative insight is required to perform single molecular or particulate analyses [1-4]. In addition, profound understanding and manipulation of biomolecule properties at nano-scale provide significant improvements of diagnostic methods such as cancer biomarker detection [5].

Recently, in molecular medicine, there has been growing interest in using molecular nucleic acid-based techniques [6, 7]. Regulatory non-coding RNAs (miRNAs) play key role in many critical biological functions. The miRNAs as robust biomarkers are applied in the emerging field of molecular medicine, especially in the cancer diagnosis and prognosis [8, 9]. Furthermore, these low-molecular-weight RNAs are effective on cellular proliferation, apoptosis [10], and down-regulation of pathogenic genes. In particular, miRNA-21 as the key oncomir is up-regulated in a variety of human cancers [10, 11], including breast [6, 7], lung [9], liver cancers [10, 12].

Gold nanorods (GNRs) as the tracking nano-particles with unique optical properties, positive surface charges and bio-interaction capabilities [13-15] can be used in the sequence-specific detection methods to identify specific biomolecules or biomarkers [16-18].

In scanning probe microscopy (SPM), the highest throughput is achieved via scanning tunneling microscopy (STM), which is associated with high atomic resolution of two and three-dimensional imaging for single particles or molecules [19, 20]. A detailed topographic map of surface changes can be precisely scanned at the nano-level to measure electrical signals of biomolecular bonds through STM [21].

This research is focused on utilizing electron tunneling effects to reach an ultra-resolution detection of miRNA-21 as a cancer biomarker at nanomolar concentrations. In this study, we would like to introduce a novel nanocharacterization method to develop diagnostic and

therapeutic nanomolecular approaches for MicroRNA with regard to structural changes of tracer nanoparticles such as GNRs.

2. Materials and Methods

2.1 Chemical reagents and analytical instruments

The rod-shaped gold nanoparticles in the forms of colloidal suspension (cat no: 716812; 10 nm in diameter) were produced from Sigma-Aldrich, Germany. In the current study, nano-topography was carried out using scanning tunneling microscopy (NAMA STM SS3-L1) and highly ordered pyrolytic graphite (HOPG) surfaces from NATSYCO, IRAN. Surface potential and size analysis were investigated through dynamic light scattering (Nano-ZS analyzer; 633 nm, Malvern Co., U.K).

The most effective sequence of human miRNA-21 (MIMAT0000790) as one of the most common cancer biomarker (5'- UAGCUUAUCAGACUGAUGUUGA -3') (22-24) was chemically synthesized and annealed by BIONEER. Co (Germany). The primary concentration of miRNA-21 is approximately $4000 \mu\text{gml}^{-1}$, but in this study, the suitable concentration of miRNA oligomers was determined to be $34 \text{ ng}\mu\text{l}^{-1}$ using a serial dilution method, absorbance unit, and gel electrophoresis.

2.2 GNR- miRNA complexation

After normalization of the solutions, suitable concentrations of GNRs (at $35 \text{ ng}\mu\text{l}^{-1}$) and miRNA-21 (at $34 \text{ ng}\mu\text{l}^{-1}$) were mixed in equal volumes, vortexed, and optimized at pH 7.4. Then, the mixture was incubated at 37°C for 25 min for an electrostatic binding to be formed between anionic miRNA oligoes and cationic surfaces of GNRs. The GNR particles were sonicated for 2 min to prevent aggregation.

2.3 Dynamic light scattering

DLS was employed to determine mean hydrodynamic diameters and surface potentials [25, 26] of GNRs, miRNA-21, and GNR-miRNA complexes. The results were obtained under the parameters such as dispersant RI 1.33, material RI 1.59, and material absorption 0.01 at pH 7.4 in a backscatter mode and then interpreted on the intensity, volume, and number distribution graphs using DTS software [27].

2.4 Scanning tunneling microscopy of rod-shaped gold nano-tracers and GNR-miRNA complexes

Morphologies, surfaces, and structures of the tracer gold nanoparticles were evaluated by the use of STM before and after the labeling of miRNA-21 as a cancer biomarker. For imaging, HOPG as a suitable sample holder (0.25 cm in thickness and 0.8 cm in diameter) with high atomic arrangement regularity [28, 29] and Rermanium tip (0.25 mm in diameter) with an atomic sharp point (30) were utilized.

After several scans, the ideal concentration of GNRs on HOPG surface was considered to be about $0.005 \mu\text{gml}^{-1}$ to form a monolayer for a high resolution imaging. Then, $10 \mu\text{l}$ of GNRs and GNR-miRNA-21 complexes were immobilized on HOPG grids and incubated at room temperature overnight for slow solvent evaporation.

STM imaging was operated in both directions to ensure that the results would not have been perturbed by the tip-sample interactions. The best resolutions of 2-D and 3-D nanographs

were taken in a constant current mode and under such electromechanical parameters as current set point (CSP): 0.2 nA, sample bias: 0.03 V, 1 kHz PID (the overall loop response time determines how fast STM can scan), and 450 pixels. Scanning was performed at a level equal to $50 \times 50 \text{ nm}$ at room temperature under ambient conditions. The topographic data were processed by NAMA-STM SS3-L1 nanoanalyzer software and low-pass filter.

2.5 Macroscopic labeling

The microtubes containing GNR and GNR-miRNA-21 were compared for macroscopic changes in transparency, homogeneity, and color.

3. Results

3.1 Dynamic light scattering

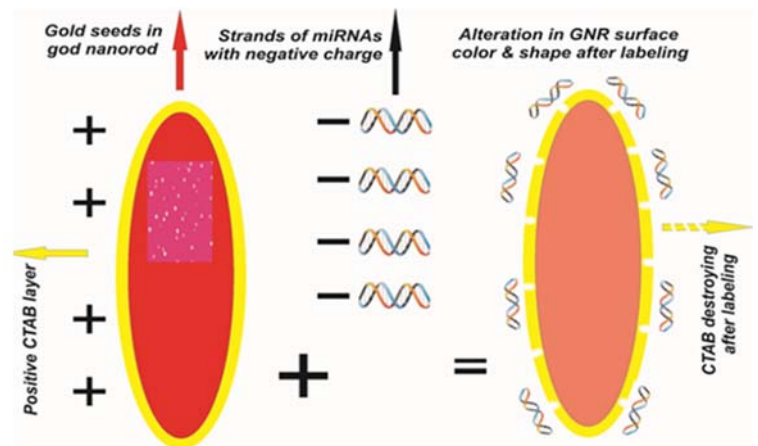
The obtained results of average hydrodynamic diameters and zeta potentials of GNRs (Figure 1), miRNA-21 (Figure 2), and GNR-miRNA-21 complexes (Figure 3) indicated significant changes illustrated in Table 1.

Table 1: DLS Parameters

Sample	Dispersant	Conductivity (ms/cm)	Viscosity (cP)
GNR	Depe water	0.0557	1.0031
miRNA	Water nuclease free	0.0395	0.8872
GNR-miRNA 21 complexes	Water nuclease free	0.148	0.8872

Table 2: Average particle size and zeta-potential of GNRs and GNR-miRNA

Sample type	Mean particle size (nm)	Zeta-potential (mV)
miRNA-21		-0.724
GNR	18.78	37.1
GNR-miRNA 21	45.91	8.39



Schematic 1: Labeling processes of miRNAs with GNRs nanotracer

This section indicates the negatively charged seeds of gold nanoparticles coating with positively charged CTAB bilayer with affinity to bioconjugate with negatively charged miRNA oligoes via non-covalent electrostatic interaction that cause to destroy of CTAB layer after sever electrostatic binding.

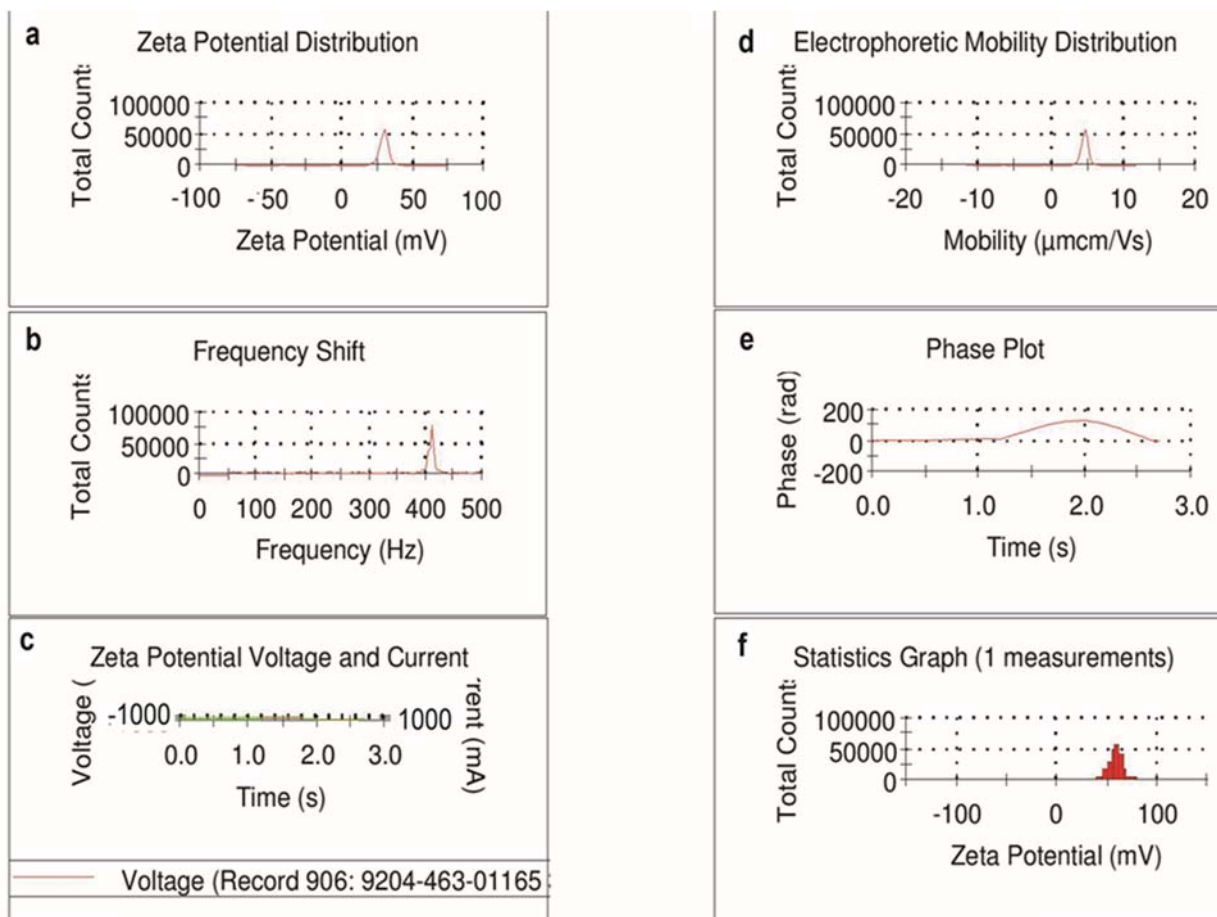


Fig 1: Zeta potential analysis of GNRs

The positive surface charge of GNRs based on their Zeta potential distribution and Electrophoretic mobility distribution.

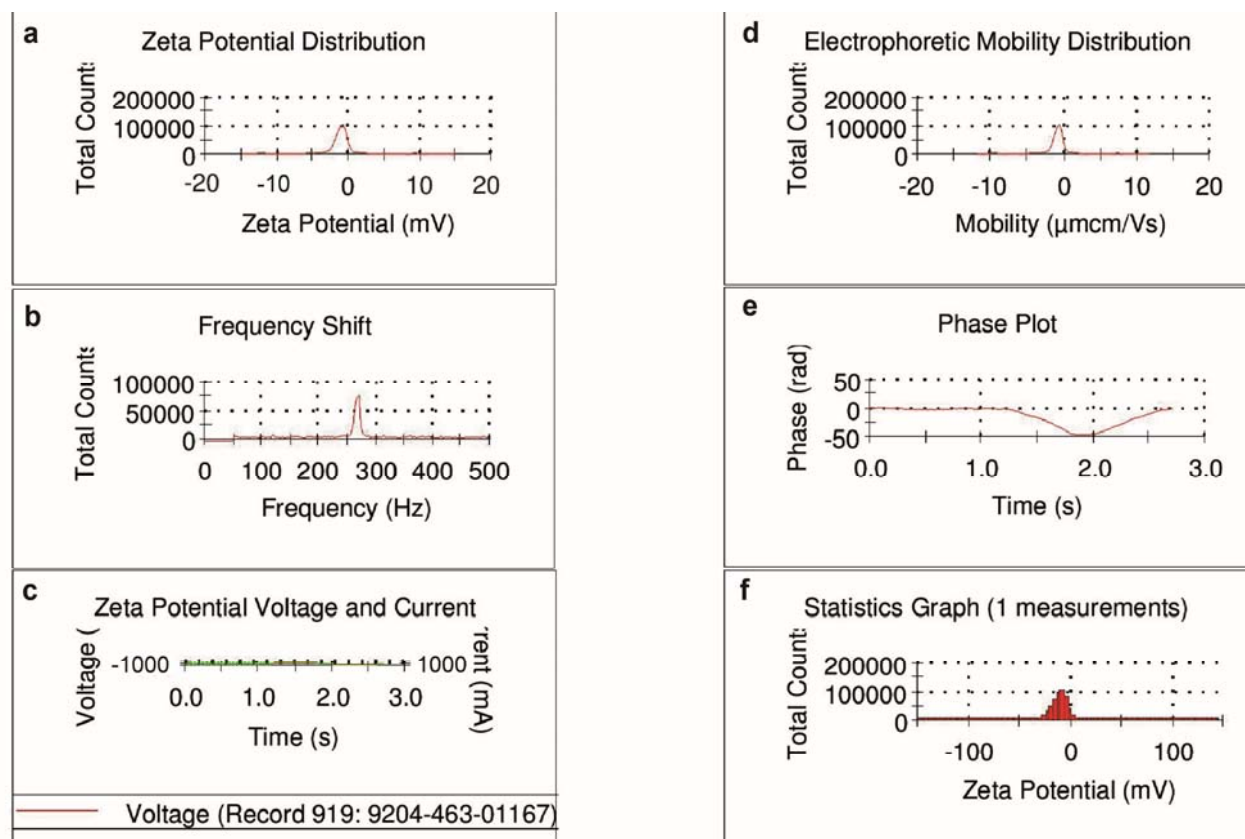


Fig 2: Zeta potential analysis of microRNA-21

The negative charge of miRNA based on their Zeta potential distribution and Electrophoretic mobility distribution.

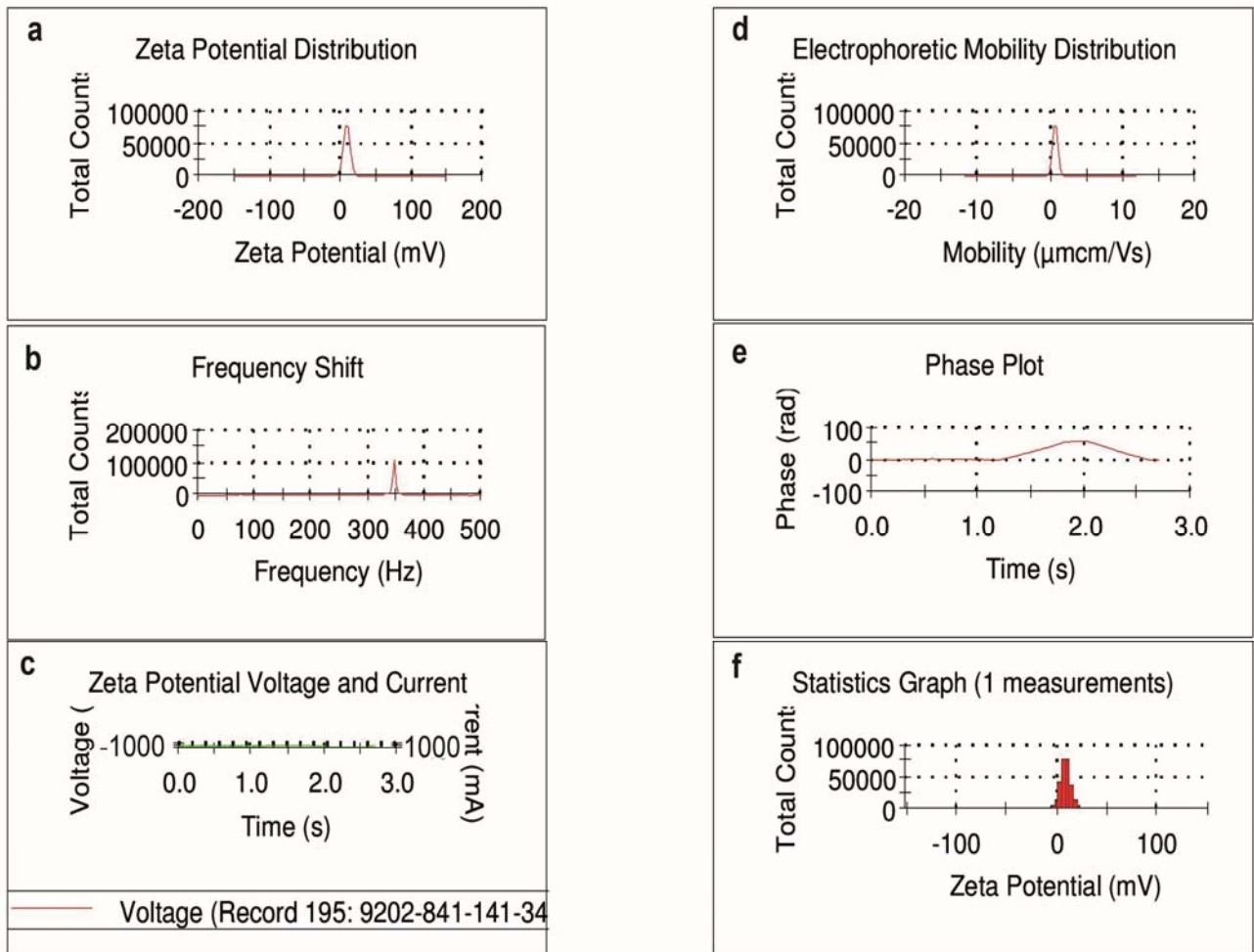


Fig 3: Zeta potential analysis of GNR-miRNA complexes after labeling phase

Reduce in positive charge of GNRs due to sever electrostatic bindings between GNRs and miRNA oligoes in complexes formation.

3.2 STM characterization of GNRs

The high-quality 2-D and 3-D nanographs of monolayer GNRs demonstrated that the morphologies of GNRs are cylindrical and uniform with regular arrangements. Size diagrams on 2-D nanographs showed regular depositions for

each gold nanoparticle. Also, the average aspect ratios of GNRs (mean length-to-width ratios of 100 GNRs) were predicted to be equal to 3 based on STM 3-D nanographs (Figure 4).

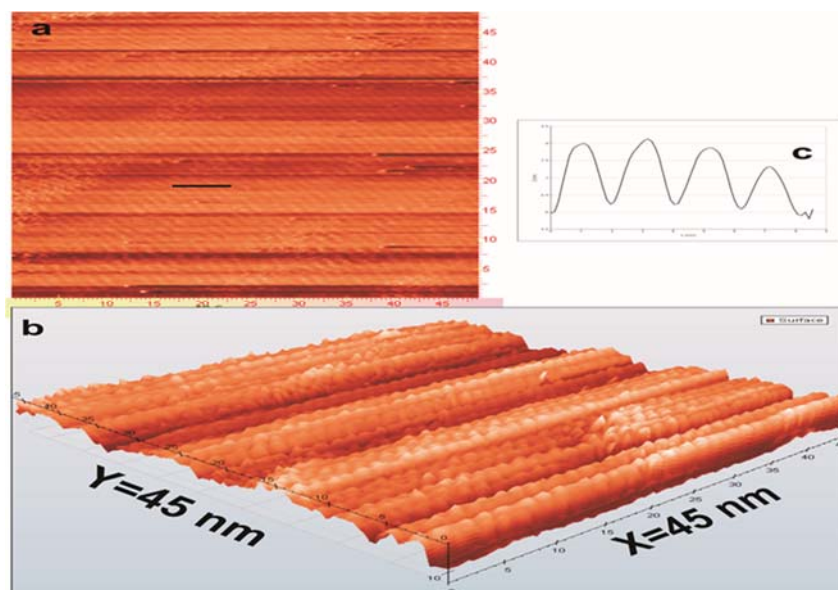


Fig 4: STM of GNRs on HOPG

2D nanograph (a); and 3D nanograph of GNRs on HOPG surface at a level equal to 45×45 nm (b); Size diagram of GNR particles on 2D nanograph (partition a) (c), respectively, diagram are demonstrated with one regular jump for each nanoparticle

3.3 STM characterization of GNRs labeled with miRNA

The nanographs of monolayer complexes (followed by miRNA addition) represented alterations in morphologies,

sizes, significant transformations, irregularities, and surface roughnesses (Figure 5).

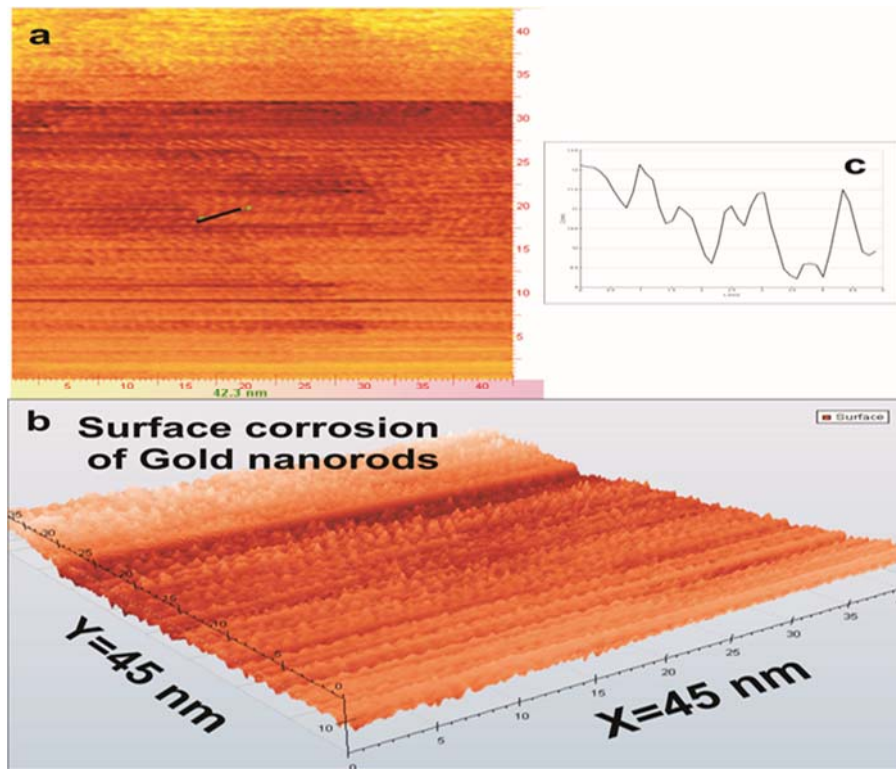


Fig 5: STM of miRNA-GNRs complexes on HOPG

2D nanograph (a); and 3D nanograph of nanoplexes on HOPG at a level equal to 45×45 nm (b); Size diagram of nanoplexes on 2D nanograph (partition a) (c). An irregular jump was showed in the diagram for each nanoplex particle.

3.4 Macroscopic labeling

The microtubes of GNRs and miRNA solutions appeared to be clear, transparent, and homogenous. The GNR was visualized as a red-pink solution, while the miRNA solution was achromatic. Within the labeling phase, after about 25 min of incubation at 37 °C, macroscopic changes in color and

accumulation were detected. As shown in Figure 6, the microtubes containing miRNA and GNRs mixtures indicated a shift from red-pink to achromatic colors. Additionally, sedimentations were observed in the microtube containing the mixture.

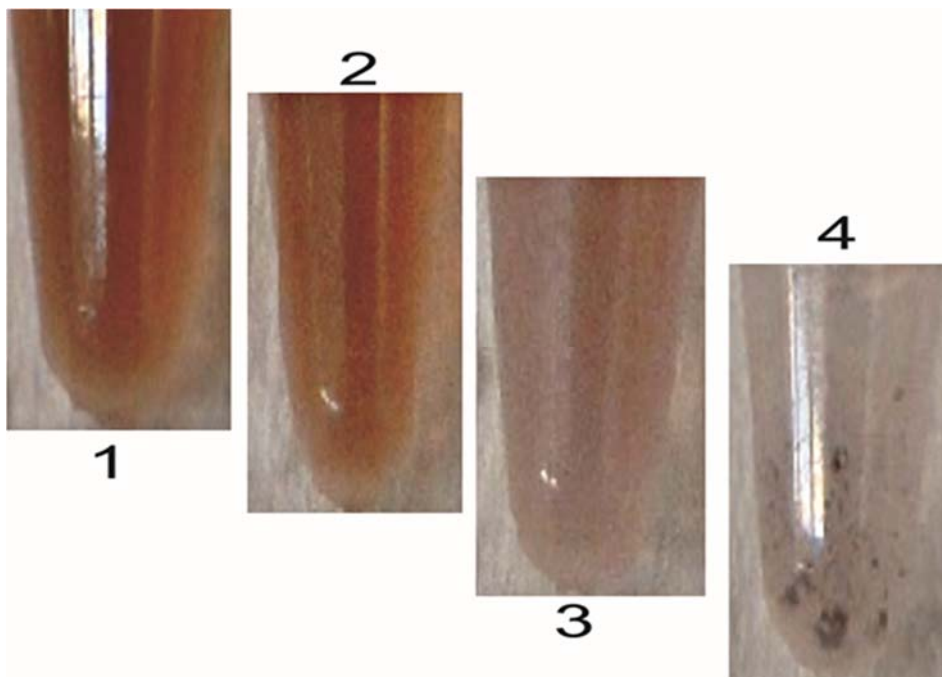


Fig 6: Colorimetric visualization

GNR solution with red color (1); Mixture of GNR-miRNA complexes after 1 min (2); After 10 min with color shifting to red-pink (3); After 20 min labeling with color shifting to achromatic and sedimentation (4).

4. Discussion

To develop molecular medicine for the diagnosis, prognosis, prevention, and treatment of severe diseases such as cancers, novel applications of advanced analytical tools are required for biomolecular identification [1-4]. Our ultimate aim was to confirm the hypothesis that advanced nanotechnology in molecular scanning can exert a significant role on the characterization and detection improvements of biomedical markers at the single-molecule level to remove the obstacles and limitations in the way of medical sciences.

In the last decade, nucleic acids, especially miRNAs, have been extensively investigated in the field of nanobiosciences. There are 3 main categories of detection methods to identify nucleic acids of various sizes as functionalized biomolecules: target amplification (polymerase chain reaction, etc) and probe amplification (ligase reaction, etc) that are frequently used today and the third group which is based on the detection of single molecular signals is referred to as signal amplification method. The common characterization techniques can analyze average populations of target samples against single-molecule analysis [31].

We first performed size and surface charge tests to investigate whether GNRs could efficiently label miRNA, indicating affinity of CTAB-coated GNR to miRNA phosphates in the complexes (Scheme 1).

As mentioned above, to achieve an accurate and detailed single-molecule evaluation directly or indirectly, employment of high-throughput equipments and advanced methods at nanoscale level is required using nanoscopy with the capability of recording single-molecule signals or scanning probe microscopy [19, 20]. To this end, STM with the capabilities of high resolution imaging, electron tunneling effect, and tracking particle behavior was conducted. The present study investigated nanomolecular events in a topographic mode. Furthermore, GNR particles were used as tracer particles. As reported in this study, this can be explained by the fact that the GNRs with cationic CTAB surfaces have significant affinities for potently labeling on anionic-surface phosphate groups of miRNA oligonucleotides through non-covalent electrostatic binding into detectable complexes. Two-surface plasmon resonances of GNRs have a major role in binding to nucleic acid molecules [13-18]. Relying on the reduction of surface charges and significant increases in the average sizes of GNRs after adding miRNA, we could prove DLS is able to provide GNR-miRNA-21 complex formation [25-27].

The miRNAs labeled by GNRs were imaged indirectly by STM with an excellent resolution on HOPG surface. The presence of biomolecules was proven indirectly following the behaviors and structural changes of GNRs after the labeling phase. When there is no binding, morphologies of the GNRs remain intact and unchanged. In addition, the presence of the targeted biomolecules can be predicted as soon as the deformation, rugosity, and corrosion of GNR surfaces are observed. Even when excessive attaching of miRNA oligomers to the GNRs occurs, numerical or electrostatic severities can cause a complete loss of nanocarrier structures.

Finally, we demonstrated that molecular confrontation at nanoscale level together with its direct effect can prove the presence of the target single molecules indirectly. Our findings facilitate achievements of optimum application and characterization of RNA molecules in molecular medicine and remove the obstacles which stand in the way of biomolecular diagnosis and treatment of severe diseases.

5. Conclusion

In this research, scanning tunneling microscopy and a new application of single biomolecule analysis of miRNA oligoes using tracer gold nanorod particles were employed to complete characterization more precisely and obtain an optimal efficacy without any concerns about their concentrations and ratios. We believe that different biomolecular behaviors are achieved at the single-molecule level.

Based on our observations, we introduced a new insight into the identification methods of functionalized biomolecules and biomarkers, such as consideration of miRNAs and their reactions with other nanomedical agents. Moreover, the results illustrated that STM as a basic nanodevice can be employed in molecular medicine processes with a major role in molecular diagnosis and treatment of cancers.

In summary, we showed that the presence of targeted single biomolecules and biomarkers can be proven indirectly by focusing on the observed direct effects of molecular confrontation at nanoscale level.

Therefore, these findings can be used to develop novel nanodiagnostic and nanotherapeutic methods, especially to characterize nanocarriers, stable siRNA delivery, and MicroRNA detection in cancer diseases.

6. Acknowledgements

The project was supported partially by Vice Iran Nanotechnology Initiative council (INIC).

7. References

1. Moghimi SM, Hunter AC, Murray JC (2005) Nanomedicine: current status and future prospects. *The FASEB Journal*. 19: 311-330.
2. Nathan DG (1996) Molecular Medicine Society: A Greet start, A Greet Future. *Molecular Medicine*. 2: 527-529.
3. Dadhich A, Sharma G, Kumar D (2012) Future effect of Nano-Medicine on human generation. *International Journal of Engineering Research and Applications (IJERA)*. 2: 7-11.
4. Poss JS, Linette GP, Clark E, Ayers M, Leschly N (2004) Breast cancer biomarkers and molecular medicine: part II. *Expert Rev Mol Diagn*. 4: 169-188.
5. Liu Y, Niu TS, Zhang L, Yang JS (2010) Review on nano-drugs. *Natural Science*. 2: 41-48.
6. Hafez MM, Hassan ZK, N Zekri AR, Gaber AA, Al Rejaie SS, Sayed (2012) MicroRNAs and Metastasis-related Gene Expression in Egyptian Breast Cancer Patients. *Asian Pacific J Cancer Prev*. 13: 591-598.
7. Qi L, Bart J, Tan LP, Platteel I, van der Sluis T (2009) Expression of miR-21 and its targets (PTEN, PDCD4, TM1) in flat epithelial atypia of the breast in relation to ductal carcinoma in situ and invasive carcinoma. *BMC Cancer*. 9:163.
8. Anastasov N, Höfig I, Vasconcellos IG, Rappl K, Braselmann H (2012) Radiation resistance due to high expression of miR-21 and G2/M checkpoint arrest in breast cancer cells. *Radiation Oncology*. 7: 206.
9. Yan LX, Huang XF, Shao Q, Huang MY, deng L (2008) MicroRNA miR-21 over expression in human breast cancer is associated with advanced clinical stage, lymph node metastasis and patient poor prognosis. *RNA*. 14: 2348-2360.
10. Frankel LB, Christoffersen NR, Jacobsen A, Lindow M, Krogh A *et al.* (2008) RNA-Mediated Regulation and Noncoding RNAs: Programmed Cell Death 4 (PDCD4)

- Is an Important Functional Target of the MicroRNA *miR-21* in Breast Cancer Cells. *J Biol Chem.* 283:1026–1033.
11. Yan LX, Wu QN, Zhang Y, Li YY, Liao DZ (2011) Knockdown of miR-21 in human breast cancer cell lines inhibits proliferation, in vitro migration and in vivo tumor growth. *Breast Cancer Research.* 13:R2.
 12. Huang GL, Zhang XH, Guo GL, Huang KT, Yang KY et.al (2009) Clinical significance of miR-21 expression in breast cancer: SYBR-Green I-based real-time RT-PCR study of invasive ductal carcinoma. *ONCOLOGY REPORTS.* 21: 673–679.
 13. Mirkin CA, Seferos D, Giliohann DA (2013) Particles for detecting intracellular targets. Publication number US8507200 B2.
 14. Kanjanawarut R, Su X (2010) Study of nucleic acid–gold nanorod interactions and detecting nucleic acid hybridization using gold nanorod solutions in the presence of sodium citrate. *Biointerphases.* 3: FA98–FA104.
 15. Ma W, Kuang H, Xu L, Ding L, Xu C (2013) Attomolar DNA detection with chiral nanorod assemblies. *NATURE COMMUNICATIONS.* DOI: 10.1038/ncomms3689.
 16. Wu J, Li W, Hajisalem G, Lukach A, Kumacheva E, Hof F, Gordon R (2014) Trace cancer biomarker quantification using polystyrene-functionalized gold nanorods. *Biomed Opt Express.* 3;5(12):4101-4107.
 17. Vigderman L, Khanal BP, Zubarev ER (2012) Functional Gold Nanorods: Synthesis, Self-Assembly, and Sensing Applications. *Adv Mater.* 24: 4811–4841.
 18. Cornejo-Monroya D, Acosta-Torres LS, Moreno-Vegac AI, Saldanad C, Morales-Tlalpan V et.al (2013) Gold nanostructures in medicine: past, present and future. *Journal of Nanoscience Letters.* 3: 25.
 19. Kano S, Tada T, Majima Y (2015) Nanoparticle characterization based on STM and STS. *Chem Soc Rev.* 21;44(4):970-87.
 20. Datar S, Kumar PM, Sastry M, Dharmadhikari CV (2004) Scanning tunneling microscopy/ spectroscopy of titanium dioxide nanoparticulate film on Au (1 1 1) surface. *Colloids and Surfaces A: Physicochem. Eng. Aspects.* 232: 11–17.
 21. Zhao K, Lv YF, Ji SH, Ma X, Chen X, Xue QK (2014) Scanning tunneling microscopy studies of topological insulators. *J Phys Condens Matter.* 1;26(39):394003.
 22. Chen Y, Zhang L, Hao Q (2013) Candidate microRNA biomarkers in human epithelial ovarian cancer: systematic review profiling studies and experimental validation. *Cancer Cell International.* 13: 86.
 23. Zhen-feng L, Yin-lin G, Jin-yu Z, Hui Z, Xiao-feng C et.al (2013) The Diagnosis value of Plasma microRNAs for Primary Breast Cancer. *Progress in Modern Biomedicine.* 27: 5310–5314.
 24. Yuan J, Chen L, Chen X, Sun W, Zhou X (2012) Identification of Serum MicroRNA-21 as a Biomarker for Chemosensitivity and Prognosis in Human Osteosarcoma. *Journal of International Medical Research.* 40:2090–2097
 25. Jamting K, Cullen J, Coleman VA, Lawn M, Herrmann J et.al (2011) Systematic study of bimodal suspensions of latex nanoparticles using dynamic light scattering. *Adv Powder Technol.* 22: 290–293.
 26. Kato H, Suzuki M, Fujita K, Horie M, Endoh Sh et.al (2009) Reliable size determination of nanoparticles using dynamic light scattering method for in vitro toxicology assessment. *Toxicol In Vitro.* 23: 927–934.
 27. Murdock RC, Braydich-Stolle L, Schrand AM, Schlager JJ, Hussain SM (2008) Characterization of nanomaterial dispersion in solution prior to in vitro exposure using dynamic light scattering technique. *Toxicol Sci.* 101: 239–253.
 28. Marz M, Sagisaka K, Fujita D (2013) Ni nanocrystals on HOPG (0001): A scanning tunnelling microscope study. *Beilstein J Nanotechnol.* 4: 406–17.
 29. Eren B, Hug D, Marot L, Pawlak R, Kisiel M et.al (2012) Pure hydrogen low-temperature plasma exposure of HOPG and graphene: Graphene formation?. *Beilstein J Nanotechnol.* 3: 852–859.
 30. Castellanos-Gomez A, Rubio-Bollinger G, Garnica M, Barja S, Vázquez de Parga AL et.al (2012) Highly reproducible low temperature scanning tunneling microscopy and spectroscopy with in situ prepared tips. *Ultramicroscopy.* 122: 1–5.
 31. Carrino JJ, Lee HH (1995) Nucleic acid amplification methods. *Journal of Microbiological Methods.* 23:3-20.